31st Annual International Conference of the IEEE EMBS
Minneapolis, Minnesota, USA, September 2-6, 2009

On Sensitivity of Molecular Specific Photoacoustic Imaging Using Plasmonic Gold Nanoparticles

Srivalleesha Mallidi, *Member, IEEE,* Pratixa P. Joshi,
Konstantin Sokolov and Stanislav Emelianov, *Member, IEEE*

***Abstract*—Functionalized gold nanospheres undergo receptor mediated aggregation on cancer cells that overexpress the epidermal growth factor receptor (EGFR). This phenomenon leads to a red shift in the plasmon resonance frequency of the EGFR-targeted gold nanoparticles. Previously we demonstrated that highly selective detection of cancer cells can be achieved using the combination of multi-wavelength photoacoustic imaging and molecular specific gold nanoparticles. In this study, we use tissue models to evaluate the sensitivity of molecular specific photoacoustic imaging in detecting cancer cells labeled with EGFR-targeted gold nanoparticles. The results of our study indicate that highly sensitive detection of cancer cells is feasible using photoacoustic imaging and plasmonic gold nanoparticles.**

***Keywords*—photoacoustic imaging, molecular imaging, bioconjugated gold nanoparticles, plasmon resonance coupling**

I. INTRODUCTION

Metal nanoparticles such as gold, silver and iron nanoparticles are being used as contrast agents in various imaging techniques [1] to facilitate early detection of cancer. Recently, gold nanoparticles (Au NPs) have gained popularity for their well-known bioconjugation protocols [2-4], biocompatibility [5, 6], and ease of tuning the optical properties [7, 8]. They have been used as nano contrast agents [9-14] for molecular imaging of neoplasms. For example, immunotargeted gold nanoparticles have been used to enhance contrast in optical imaging techniques [10-12, 14]. However, the penetration depth achievable with high resolution optical imaging techniques is limited to a few millimeters. Photoacoustic imaging, on the other hand, can provide a penetration depth on the order of centimeters if near-infrared (NIR) laser light is used [15-17]. In the photoacoustic phenomenon, electromagnetic energy in the form of light is absorbed and subsequently an acoustic wave is emitted. Using an ultrasound detector, the acoustic waves can be detected and spatially resolved to form an image of the photo absorbers in the tissue [15-17].

EGFR is upregulated in many epithelial cancers, making it a useful target for cancer detection [18, 19]. When targeted gold nanoparticles bind to EGFR they tend to cluster in the same spatial distribution as the receptors, which are known to form closely spaced assemblies upon activation followed by endocytoses of the receptors [20]. The receptor-mediated aggregation of Au NPs causes plasmon coupling of the clustered nanoparticles, leading to an optical red-shift of the plasmon resonances and an increase in absorption in the red region [10, 11]. Utilizing these changes in optical properties, we previously demonstrated that highly selective detection of cancer could be achieved using molecular targeted Au NPs and combined photoacoustic and ultrasound imaging [9].

In this study we evaluated the detection limit of photoacoustics by imaging cancer cells labeled with anti-EGFR targeted gold nanoparticles. Indeed, it is essential to estimate the sensitivity of the molecular specific photoacoustic imaging technique in tissue models prior to conducting in-vivo experiments; i.e., the minimum concentration of labeled cells or Au NPs required to observe photoacoustic response needs to be determined.

II. MATERIALS AND METHODS

The gold nanoparticles used in this study were prepared using citrate reduction of tetrachloroauric (III) acid (HAuCl4) under reflux [4]. The citrate reduction method yielded spherical gold nanoparticles with 50 nm diameter.

The protocol for antibody conjugation to gold nanoparticles has been described elsewhere [4]. Briefly, the carbohydrate moieties on the Fc region of the Ab were oxidized to aldehyde groups by addition of 100 mM $NaIO_4$ to a 1 mg/mL anti-EGFR antibodies solution in HEPES (1:10 by volume). The antibodies (Ab) were then allowed to react with a hydrazide PEG di-thiol heterobifunctional linker (Sensopath Technologies, Inc.), where the hydrazide portion of the linker covalently bonded to the aldehyde groups on the antibody, yielding exposed di-thiol moieties that could react strongly with the gold nanoparticles. The Ab-linker was centrifuged using 100 kDa MWCO centrifugal filter (Amicon) and resuspended in 40 mM HEPES (pH = 8) mL. The Ab-linker solution was mixed with gold nanoparticles (Au NPs). mLreacted on a shaker for 20 min at room temperature. Any remaining bare gold surface was capped with mPEG-SH (5 kD, Creative PEGWorks) and the conjugated particles were collected as a pellet after centrifugation at 2500 g for 30 minutes. The EGFR-targeted Au NPs were filter sterilized (0.2 μm pore size, Corning) before mixing with cells. The unlabeled and labeled cells were characterized using darkfield optical imaging.

Tissue mimicking phantoms were made with gelatin containing different concentrations of human epithelial carcinoma cells (A431 keratinocyte) labeled with anti-EGFR Au NPs. Specifically, cells labeled with anti-EGFR Au NPs were prepared at a $1x10^7$ cells/mL concentration using the

Manuscript received April 23, 2009. This work was supported in part by the National Institutes of Health under grants EB008101 and EB004963.

S. Mallidi, P. Joshi and S. Emelianov* are with the Department of Biomedical Engineering, University of Texas at Austin, Austin, TX 78712 USA (*corresponding authors: 512-471-1733; fax: 512-471-0616; e-mails: emelian@mail.utexas.edu).

K. Sokolov is from Department of Imaging Physics, University of Texas M.D. Anderson Cancer Center, Houston, TX 77030

procedure described previously [9]. The cell suspension was mixed with different volumes of gelatin solution (10% by weight) to obtain a range of Au NPs concentration. The cell/gelatin solutions (100 µL) with different concentrations of nanoparticles were pipetted into separate spacers for imaging. After the imaging experiments, the cell/gelatin samples were extracted from the spacers and dissolved in 1% nitric acid for quantitative determination of Au NPs concentration using inductively coupled plasma mass spectroscopy (ICP-MS).

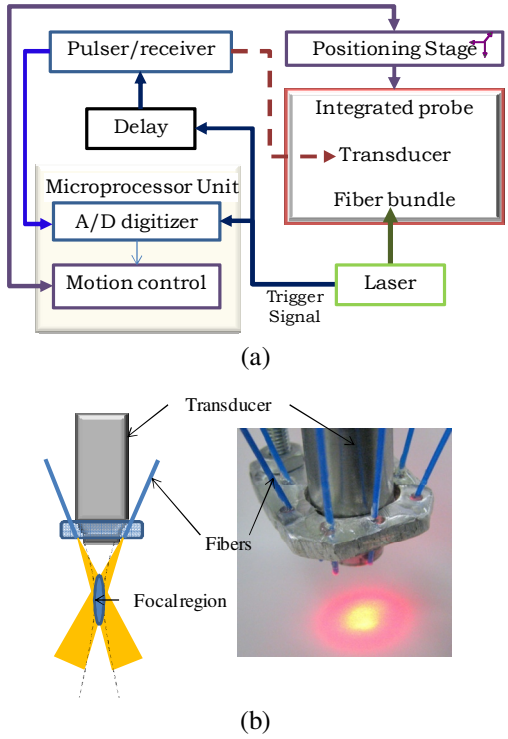

Fig. 1: (a) Block diagram of the combined ultrasound and photoacoustic imaging system. (b) Schematic representation and photograph of the integrated imaging probe consisting of 25 MHz ultrasound transducer and seven 600 µm diameter optical fibers.

The ultrasound and multi-wavelength photoacoustic imaging of the cell/gelatin solutions were performed using an integrated photoacoustic and ultrasound imaging system, presented in Fig. 1a. The imaging system consists of a microprocessor unit with a custom built LabVIEW application that controls the ultrasound pulser/receiver, pulsed laser, data acquisition unit, and all motion axes needed for 3-D mechanical scanning. A 25 MHz single element focused (focal depth = 25.4 mm, f# = 4) ultrasound transducer was used to obtain both ultrasound and photoacoustic images of the tissue phantoms. A tunable OPO laser system operating at 720 nm wavelength (7 ns pulse duration, 10 Hz pulse repetition frequency) was used to generate photoacoustic transients. The laser irradiation was delivered via optical fiber bundle consisting of seven 600 µm diameter fibers. On the proximal end of the bundle, all the fibers arranged in a circular configuration were coupled to a laser beam. On the distal end, the fibers were distributed around and attached to the transducer such that the focal region of the ultrasound transducer and the optical beams from the fibers coincided spatially (Fig. 1b). This integrated probe was attached to the motion axis to allow the mechanical scanning of the tissue phantoms.

During offline processing, the photoacoustic and ultrasound signals were extracted from the A-line records obtained at each lateral step of the mechanical scan. A digital bandpass (5-45 MHz) filter was applied to these raw radiofrequency (RF) signals to reduce noise. A Hilbert transform was applied to the filtered RF data to obtain ultrasound and photoacoustic analytic signals. Finally, the signals were spatially interpolated and displayed.

III. Results and Discussion

The darkfield images of the unlabeled and labeled cells are shown in Fig. 2a and Fig. 2b, respectively. The unlabeled cells appear bluish regions in the darkfield image (Fig. 2a) due to their intrinsic light scattering properties. The targeted cells (Fig. 2b) appear orange colored cells due to the plasmon-resonance scattering of anti-EGFR conjugated gold nanoparticles which interact with EGFR molecules on the cytoplasmic membrane of the cancer cells.

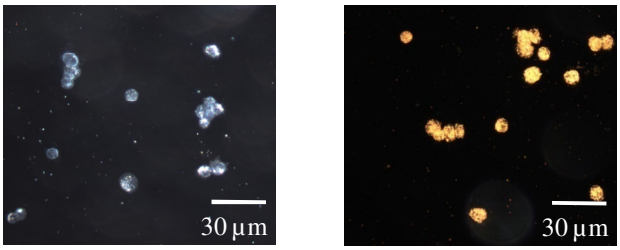

Fig. 2: Darkfield images of A431 cells with (a) no gold nanoparticles and (b) anti-EGFR conjugated gold nanoparticles.

The ultrasound and photoacoustic images of the cell/gelatin tissue models are shown in Fig. 3. The photoacoustic images were obtained at 720 nm wavelength illumination. The concentrations of the Au NPs obtained from ICP-MS analysis as well as the concentrations of the cells in gelatin samples are also given in Fig. 3. A decrease in the amplitude of the backscattered echo in ultrasound images (Figs. 3a-3d) clearly indicates a decrease in the concentration of cells in the samples. It can also be observed in Figs. 3e-3h that the photoacoustic signal amplitude decreases as a function of cell/Au NPs concentration.

The amplitude of the photoacoustic signal is proportional to the optical absorption coefficient of the tissue constituents and the input laser fluence. Therefore, a change in the concentration of Au NPs in the tissue will affect the strength of the photoacoustic transients generated in the tissue. Specifically, a 2 mm by 1 mm region of interest was chosen for each cell/gelatin sample image (Figs. 3e-3h) and divided into 200 subareas measuring 0.1 mm x 0.1 mm. The mean and the standard deviation of the photoacoustic signal amplitude was calculated and plotted as a function of Au NPs concentration in Fig. 4. A linear regression fit of the data yielded an R^2 value equal to 0.99. This result was expected; given the constant laser input fluence and the fact that the amplitude of the photoacoustic signal is proportional to the absorber (Au NPs) concentration. The detection limit for the photoacoustic imaging technique was ~ 3 x 10^4 cells/mL or ~ 3 x 10^7 Au NPs/mL. Note that the

experiments were performed at a fluence of 5 mJ/cm^2 – this value is less than the ANSI standard of the maximum allowable fluence (20 mJ/cm^2) for pulsed lasers [16].

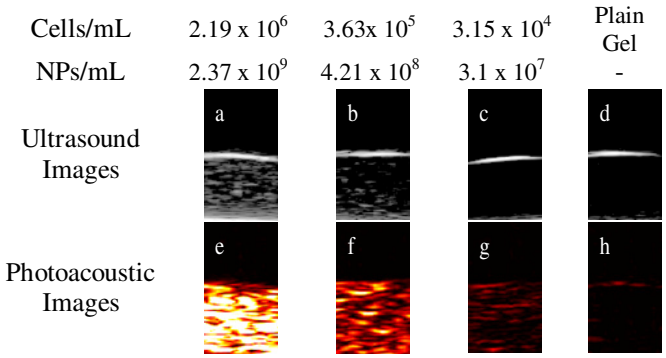

Fig. 3: The ultrasound (a-d) and photoacoustic (e-h) images of cell/gelatin samples at different cell concentration. The photoacoustic images were obtained at 720 nm wavelength illumination. The images measure a 2 mm by 3.5 mm field of view.

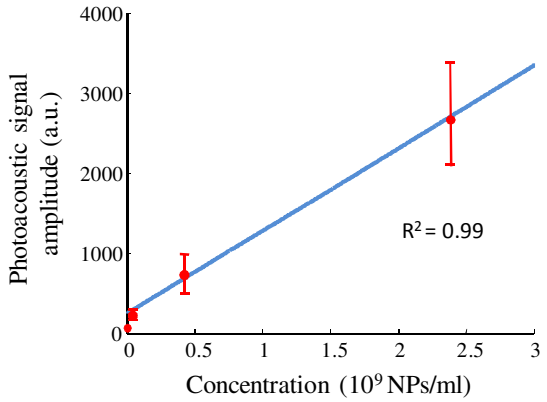

Fig. 4: Graph depicting the change in photoacoustic signal amplitude with Au NPs concentration. The solid line represents the linear regression fit of the data with R^2 equal to 0.99.

IV. Conclusion

Epidermal growth factor receptor (EGFR) is overexpressed in various epithelial tumors. A red shift in the plasmon resonance frequency of the EGFR-targeted gold nanoparticle assembly can be observed due to plasmon resonance coupling between clustered anti-EGFR conjugated gold nanoparticles [10-12]. Based on this phenomena, we previously demonstrated on tissue models that highly selective detection of cancer could be achieved using molecular targeted gold nanosensors and combined photoacoustic and ultrasound imaging [9]. In this study, we evaluated the sensitivity of the photoacoustic imaging technique in detecting cancer cells labeled with bioconjugated gold nanoparticles. Further studies are required to evaluate the sensitivity of in-*vivo* molecular specific imaging; and subsequently, combining imaging with phototherapy to enhance the current therapeutic techniques.

Acknowledgments

The authors would like to thank Mr. Timothy Larson, Ms. Justina Tam and Mr. Andrei Karpiouk of the University of Texas at Austin for their valuable suggestions regarding the experimental setup.

References

[1] S. A. Wickline and G. M. Lanza, "Nanotechnology for molecular imaging and targeted therapy," *Circulation,* vol. 107, pp. 1092-5, Mar 4 2003.

[2] G. T. Hermanson, *Bioconjugate techniques*. San Diego, CA: Academic, 1996.

[3] M. Horisberger, "Colloidal gold: a cytochemical marker for light and fluorescent microscopy and for transmission and scanning electron microscopy," *Scan. Electron Microsc,* vol. 2, pp. 9-31, 1981.

[4] S. Kumar, J. Aaron, and K. Sokolov, "Directional conjugation of antibodies to nanoparticles for synthesis of multiplexed optical contrast agents with both delivery and targeting moieties," *Nat Protoc,* vol. 3, pp. 314-20, 2008.

[5] M. Hayat, *Colloidal gold: Principles, methods and aapplications*. San Diego, CA: Academic, 1989.

[6] E. E. Connor, J. Mwamuka, A. Gole, C. J. Murphy, and M. D. Wyatt, "Gold nanoparticles are taken up by human cells but do not cause acute cytotoxicity," *Small,* vol. 1, pp. 325-7, Mar 2005.

[7] S. J. Oldenburg, R. D. Averitt, S. L. Westcott, and N. J. Halas, "Nanoengineering of optical resonances," *Chem. Phys. Lett.,* vol. 288, pp. 243-247, 1998.

[8] J. Yguerabide and E. E. Yguerabide, "Resonance light scattering particles as ultrasensitive labels for detection of analytes in a wide range of applications," *J. Cell. Biochem,* vol. 84, pp. 71-81, 2001.

[9] S. Mallidi, T. Larson, J. Aaron, K. Sokolov, and S. Emelianov, "Molecular specific optoacoustic imaging with plasmonic nanoparticles," *Opt. Express* vol. 15, pp. 6583-6588 2007.

[10] J. S. Aaron, N. Nitin, K. Travis, S. Kumar, T. Collier, S. Y. Park, M. José-Yacamán, L. Coghlan, M. Follen, R. Richards-Kortum, and K. V. Sokolov, "Plasmon resonance coupling of metal nanoparticles for molecular imaging of carcinogenesis in vivo," *J. Biomed. Opt.,* vol. 12, p. 034007, 2007.

[11] K. Sokolov, M. Follen, J. Aaron, I. Pavlova, A. Malpica, R. Lotan, and R. Richards-Kortum, "Real-time vital optical imaging of precancer using anti-epidermal growth factor receptor antibodies conjugated to gold nanoparticles," *Cancer Res.,* vol. 63, pp. 1999-2004, May 1 2003.

[12] K. Sokolov, J. Aaron, B. Hsu, D. Nida, A. Gillenwater, M. Follen, C. MacAulay, K. Adler-Storthz, B. Korgel, M. Descour, R. Pasqualini, W. Arap, W. Lam, and R. Richards-Kortum, "Optical systems for in vivo molecular imaging of cancer," *Technol. Cancer Res. Treat.,* vol. 2, pp. 491-504, Dec 2003.

[13] J. A. Copland, M. Eghtedari, V. L. Popov, N. Kotov, N. Mamedova, M. Motamedi, and A. A. Oraevsky, "Bioconjugated gold nanoparticles as a molecular based contrast agent: Implications for imaging of deep tumors using optoacoustic tomography," *Mol. Imaging Biol,* vol. 6, pp. 341-349, 2004.

[14] C. Loo, A. Lin, L. Hirsch, M. H. Lee, J. Barton, N. Halas, J. West, and R. Drezek, "Nanoshell-enabled photonics-based imaging and therapy of cancer," *Technol Cancer Res Treat,* vol. 3, pp. 33-40, Feb 2004.

[15] A. Oraevsky and A. Karabutov, "Optoacoustic Tomography," in *Biomedical Photonics Handbook*. vol. PM125, chapter 34, T. Vo-Dinh, Ed.: CRC Press, 2003, pp. 34/1-34/34.

[16] M. Xu and L. V. Wang, "Photoacoustic imaging in biomedicine," *Rev. Sci. Instrum,* vol. 77, p. 041101, 2006.

[17] S. Y. Emelianov, S. R. Aglyamov, A. B. Karpiouk, S. Mallidi, S. Park, S. Sethuraman, J. Shah, R. W. Smalling, J. M. Rubin, and W. G. Scott, "Synergy and applications of combined ultrasound, elasticity, and photoacoustic imaging," *in Proceedings of the IEEE International Ultrasonics Symposium,* pp. 405-415, October 3-6 2006.

[18] R. Todd and D. T. W. Wong, "Epidermal growth factor receptor (EGFR) biology and human oral cancer," *Histol. Histopathol.,* vol. 14, pp. 491-500, 1999.

[19] C. Barnes and R. Kumar, "Biology of the Epidermal Growth Factor Receptor Family," in *Molecular Targeting and Signal Transduction*, 2004, pp. 1-13.

[20] D. S. Lidke, P. Nagy, R. Heintzmann, D. J. Arndt-Jovin, J. N. Post, H. E. Grecco, E. A. Jares-Erijman, and T. M. Jovin, "Quantum dot ligands provide new insights into erbB/HER receptor-mediated signal transduction," *Nat Biotechnol,* vol. 22, pp. 198-203, Feb 2004.